Deep fluids can facilitate rupture of slow-moving giant landslides as a result of stress transfer and frictional weakening

Frédéric Cappa,[1] Yves Guglielmi,[2] Sophie Viseur,[2] and Stéphane Garambois[3]

[1] Landslides accommodate slow, aseismic slip and fast, seismic rupture, which are sensitive to fluid pressures and rock frictional properties. The study of strain partitioning in the Séchilienne landslide (France) provides a unique insight into this sensitivity. Here we show with hydromechanical modeling that a significant part of the observed landslide motions and associated seismicity may be caused by poroelastic strain below the landslide, induced by groundwater table variations. In the unstable volume near the surface, calculated strain and rupture may be controlled by stress transfer and friction weakening above the phreatic zone and reproduce well high-motion zone characteristics measured by geodesy and geophysics. The key model parameters are friction weakening and the position of groundwater level, which is sufficiently constrained by field data to support the physical validity of the model. These results are of importance for the understanding of surface strain evolution under weak forcing. **Citation:** Cappa, F., Y. Guglielmi, S. Viseur, and S. Garambois (2014), Deep fluids can facilitate rupture of slow-moving giant landslides as a result of stress transfer and frictional weakening, *Geophys. Res. Lett.*, *41*, doi:10.1002/2013GL058566.

1. Introduction

[2] Fluids are known to be a triggering and driving factor for landslides. Hydromechanical coupling has been proposed as possible explanation for landslide dynamics, including both slow, aseismic slip and fast, seismic rupture [*Cappa et al.*, 2004; *Guglielmi et al.*, 2005; *Gaffet et al.*, 2010; *Viesca and Rice*, 2012]. The widely accepted understanding is that rainfall, snowmelt, and the seasonality of the groundwater recharge increase fluid pressures, which, in turn, reduce effective stress, and thus alter the strength of rocks and rupture surfaces, promoting sliding [*Iverson*, 2005]. Most evidence for fluids affecting the stability of large rock slopes comes from indirect observations based on hydrogeology and hydrogeochemistry [*Guglielmi et al.*, 2002], as well as from the correlations between rainfall and seismic activity [*Spillmann et al.*, 2007; *Helmstetter and Garambois*, 2010]. So far, most interpretations focused on the effects of rainfall

infiltration into landslides and did not investigate in detail the role of groundwater table variations below the landslides on the rupture processes. However, such considerations are important, since observations of well-documented giant landslides showed that the moving volume extends hundreds of meters above the slope aquifer (for example, the Randa landslide in Switzerland [*Willenberg et al.*, 2008]). Furthermore, although motions correlate well with seasonal infiltrations, no significant pore pressure increase has ever been measured within the landslide body, particularly in high-permeability rocky landslides. Indeed, motions occur in the near surface of the unsaturated slope, which is, in general, highly permeable (which allows high infiltration rates), perched, highly discontinuous, size limited, and experiences low-magnitude pore pressure buildup that is not high enough to significantly vary the effective stresses in the slope [*Guglielmi et al.*, 2002]. Triggering of local instabilities by such perched, low-pressure zones may be possible only at the critical stress level of the rock but do not explain the slow increase in the permanent background seasonal accelerations and decelerations that affect the entire landslide [*Cappa et al.*, 2004]. Thus, clarifying the role of fluids, especially the effects of groundwater table variations within the deep aquifer on the unsaturated slope slow rupture, is important for improved understanding of weak forcing mechanisms on landslides and risk assessment.

[3] Based on high-resolution multiparameter monitoring of the Séchilienne landslide (France) that is extensively instrumented with meteorological stations, springs hydrochemistry, piezometers, seismometers, extensometers, and distancemeters, we show that the groundwater recharge in the deep elastic part of the slope can facilitate rupture in the shallow unsaturated broken volume through the mechanisms of stress transfer and friction weakening. We modeled slope deformation using a hydromechanical model, including three-dimensional (3-D) topography, effective stress, and Mohr-Coulomb plasticity. The model provides a good match to the overall shape of the ruptured volume imaged by geology and seismic tomography. Our study implies that the deep poroelastic strain from groundwater table variations can be an important source of seasonal variations in landslide rerupturing and strain records.

2. Field Evidence for the Effects of Deep Fluids on the Mechanics of the Séchilienne Landslide

[4] The Séchilienne landslide is located in the southwestern part of the Belledone Crystalline Massif (Figures 1a and 1b). It has been active for a few decades along a steep slope (~40°) and has been instrumented since 1985 [*Helmstetter and Garambois*, 2010]. The current very active volume of this landslide is estimated to be up to 5 million m³, located on the border of a slowly moving mass reaching 60 ± 10 million m³
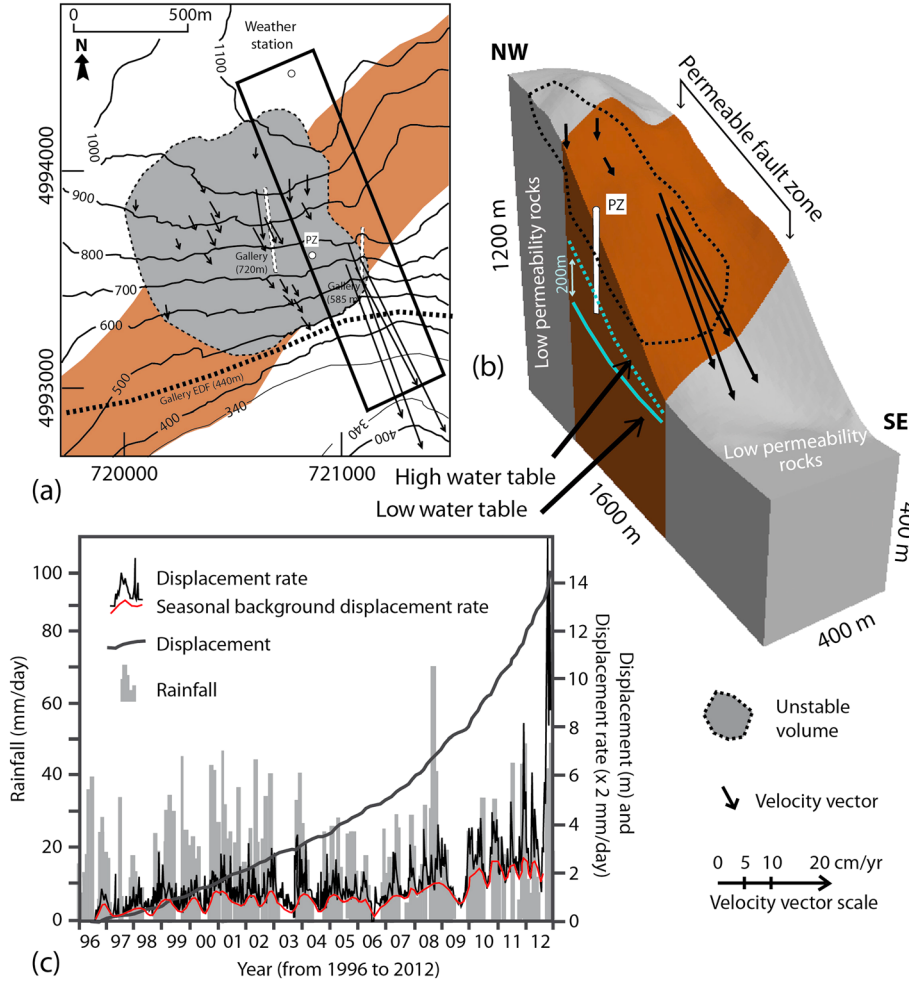
Figure 1. (a) Simplified geological map showing the location of the Séchilienne landslide and the displacement vectors. The black solid rectangle on the map illustrates the location of the (b) three-dimensional view of the high-motion zone and the position of water table (PZ is the piezometer). (c) Pluriannual variations of landslide motions compared to effective rainfall events. (Detrended seasonal variations were obtained from *Vallet et al.* [2013]).

[*Le Roux et al.*, 2011]. In the most active zone, which is also the most seismogenic region of the slope [*Lacroix and Helmstetter*, 2011], landslide displacement rates increase nonlinearly from 0.2 m/yr in 1996 to more than 2 m/yr in 2012 (Figure 1c). The other regions exhibit quasi steady state displacements generally lower than 10 cm/yr. We observe clear correlation between landslide displacement rate and effective rainfall infiltration which is characterized by a fast (few hours) delayed response of the landslide to effective rainfall infiltration events and by a delayed background permanent seasonal motion with maximum rates that is 50–70% lower in the dry season compared to the wet season (Figure 1c).

[5] The landslide is situated within a large (~700 m), near-vertical fault zone with intensively fractured rocks mainly composed of micaschists (Figures 1a and 1b) [*Meric et al.*, 2005; *Le Roux et al.*, 2011]. Outside the fault zone, the rocks are less fractured. Deep geophysical imaging determined a complex shape of the moving volume characterized by thickness variations of 100–200 m and a rough estimation of porosity of 4–30% deduced from seismic *P* wave velocities [*Le Roux et al.*, 2011].

[6] In the fault zone, *Guglielmi et al.* [2002] showed the landslide nests in several 100 m thick unsaturated zones

above the phreatic zone (Figure 1b). In the landslide, hydrochemistry of infiltration waters and flow rate variations were monitored with high resolution in two horizontal hectometer-long galleries located at the elevations of 585 and 720 m and in one vertical 150 m deep borehole drilled through the landslide body down to the deep aquifer (Figure 1a). Infiltrated meteoric waters flow vertically through fractures and shear zones, with directions N60 and N140 into the deep saturated zone. The piezometric level oscillations are estimated to be about 100 m after long-term water recharge. Waters flow rapidly, in a few hours to a few days, at small rates of maximum 0.2 L/min, and no permanent flow or pore pressure was recorded [*Vallet et al.*, 2013].

[7] The borehole allows estimating the maximum piezometric level in the basal aquifer at 629 m depth, that is, 100–200 m below the landslide boundary (Figure 1b). A gallery located at the toe of the slope (EDF gallery at the elevation of 440 m in Figure 1a) in the deep aquifer shows that outside the fault zone, there is no permanent phreatic zone due to the low permeability of the unfaulted rocks (Figures 1a and 1b). Consequently, the slope can be divided into two hydraulic regimes: a permanently saturated, deep basal aquifer within the permeable fault zone ($k \sim 9.5 \times 10^{-7}$ m/s,

deduced from hydraulic tests in the borehole), which is bounded laterally, above and below, by two low permeable, unsaturated zones ($k < 10^{-9}$ m/s) (Figure 1b).

[8] There is a paradox since geodetic and hydrogeological measurements clearly show that the landslide is mainly controlled by seasonal water infiltrations (Figure 1c), although the landslide body remains dry and unsaturated almost all year long [*Guglielmi et al.*, 2002; *Helmstetter and Garambois*, 2010]. Indeed, rapid infiltration events may explain rapid slope motions, but infiltrated waters do not remain long enough in the unsaturated destabilized volume to explain the background permanent seasonal motions, which may be related to deep permanent aquifer oscillations [*Guglielmi et al.*, 2002].

3. Coupled Fluid Pressure and Deformation Modeling

[9] Motivated by these field data, we address the general question of whether deep groundwater variations can influence the shallow slope deformations, using hydromechanical simulations. The key questions are to what extent these deep pore pressure variations may be a driving mechanism for the slow motions of shallow giant landslides and how a water table increase can affect the deformation and rupture patterns. The finite-difference code, FLAC^{3D} [*Itasca Consulting Group*, 2006], was used to model the interactions between deformation and fluid pressure in the Séchilienne landslide.

[10] In our numerical analysis, we use a block of 1.6 km × 0.4 km × 1.25 km and a 700 m wide fault zone between two less fractured rock zones, according to field observations (Figure 1b). The transition zone between the landslide and the stable part identified by seismic tomography is not represented in the initial geometry because its location and shape are control parameters for model comparison with observations. The 3-D topography and mesh were built with the GOCAD grid generator (http://www.gocad.org/w4/) and then transferred into FLAC^{3D}. To create this initial topography, we have smoothed the current topography (derived from the existing digital elevation model, available with a spatial resolution of 10 m), removing slope movements. The topography is free to move in the model, whereas no displacements were allowed perpendicular to the bottom boundary, and the natural stress gradient was set to the lateral boundaries. The modeling procedure consists of two stages: first, the model was run under gravity and without fluids, in order to reach the initial stresses before hydraulic loading is applied (Figure S1 in the supporting information). Second, after the steady state initial conditions were set, the water table is applied in the fault zone as observed in the field, and the evolution of the fluid pressure, stress, and deformation of the slope is investigated. Fluid pressure is increased progressively from the base to the middle of the slope, in order to simulate the effects of the deep aquifer seasonal oscillations. Rocks outside the fault zone are considered to be elastic, whereas elastoplastic behavior is considered for the fault zone, including an anisotropic Mohr-Coulomb model (ubiquitous joints, [*Cappa and Rutqvist*, 2011]), obeying frictional weakening from a static friction coefficient of 0.6 to a residual value of 0.2 over a critical plastic strain of 1×10^{-3}, consistent with the weakening model commonly used for landslides modeling [*Viesca and Rice*, 2012]. The ubiquitous-joint model accounts for the presence of an orientation of weakness in

the Mohr-Coulomb model. Here we assume weakness with a dip angle of 90° to represent the near-vertical fractures measured in the fault zone. We assume homogeneous rock elastic properties and porosity for the entire model (Young's modulus of 60 GPa, Poisson's ratio of 0.3, porosity of 0.1; mean values estimated in the field and in the laboratory). This setup allows us to investigate the qualitative consequences of the groundwater table variations without the additional complexity associated with the landslide geometry and bulk properties.

4. Model Results

[11] Calculated deep groundwater seasonal oscillations reproduce a range of observations for both the deformation and the rupture geometry (Figure 2). The pattern of surface displacements coincides remarkably with the areas of measured significant motions (Figure 2a), where calculated displacement magnitudes of 0.08 m are of the same order of the measured magnitudes of 0.2 m/yr. We explain the difference between the calculated and measured values by the simplified step loading adopted in the model that did not reproduce the detailed variations of the displacement rates, as well as by the effects of fast intra-annual infiltration events on slope motions that were not considered in the model (Figure 1c). Nevertheless, the current model shows that pore pressure effects in the deep aquifer resolve at least 40% of the total motions measured at the slope surface. In the model, a high–shear strain zone of maximum magnitudes of 2.3×10^{-4} develops in the shallow part of the slope, which corresponds in the field to the high porous landslide body boundaries defined by the deep geophysical imaging [*Le Roux et al.*, 2011] (Figure 2b) and by the microearthquakes focusing zone [*Lacroix and Helmstetter*, 2011] (Figure 2c). The calculated ruptured zone is larger than the landslide body deduced from surface geodesy and deep geophysics (Figure 2c). A transition zone experiencing both tensile and shear rupture separates the zones of pure tensile rupture, which is localized in the shallow part of the slope, from the zones of pure shear rupture localized deeper in the slope. The limit of the landslide body deduced from seismic tomographies matches the limit of the shallow pure tensile rupture zone. The deeper mixed tensile-shear and pure shear rupture zones that extend between this limit and the deep groundwater table location are not imaged by the available seismic tomographies, and microearthquakes rarely occur within these zones, even if their depth estimations can present large uncertainties due to the simple seismic velocity used in the location inversion [*Lacroix and Helmstetter*, 2011].

[12] The inferred landslide deformations are explained by stress changes and weakening, as illustrated by the comparison of profiles of changes in fluid pressure, stress, strain, and friction presented in Figure 3 for three positions (upstream, middle, and downstream) across the unstable zone and by the comparison with a model without weakening (i.e., constant friction) (Figure S2 in the supporting information). In the slope, the fluid pressure increase (Figure 3a) induces stress change both inside and above the phreatic zone (Figures 3b–3d) and friction weakening in the ruptured parts (Figures 3e and 3f). Below the water table and several tens to hundreds of meters above in the dry zone, the horizontal and vertical stresses reduce by 0.01–0.55 MPa, with a larger drop for the vertical component (Figures 3b and 3c), while the shear stress increases from 0.01 to a maximum of 0.13 MPa (Figure 3d). At the base of the ruptured zone, the relative
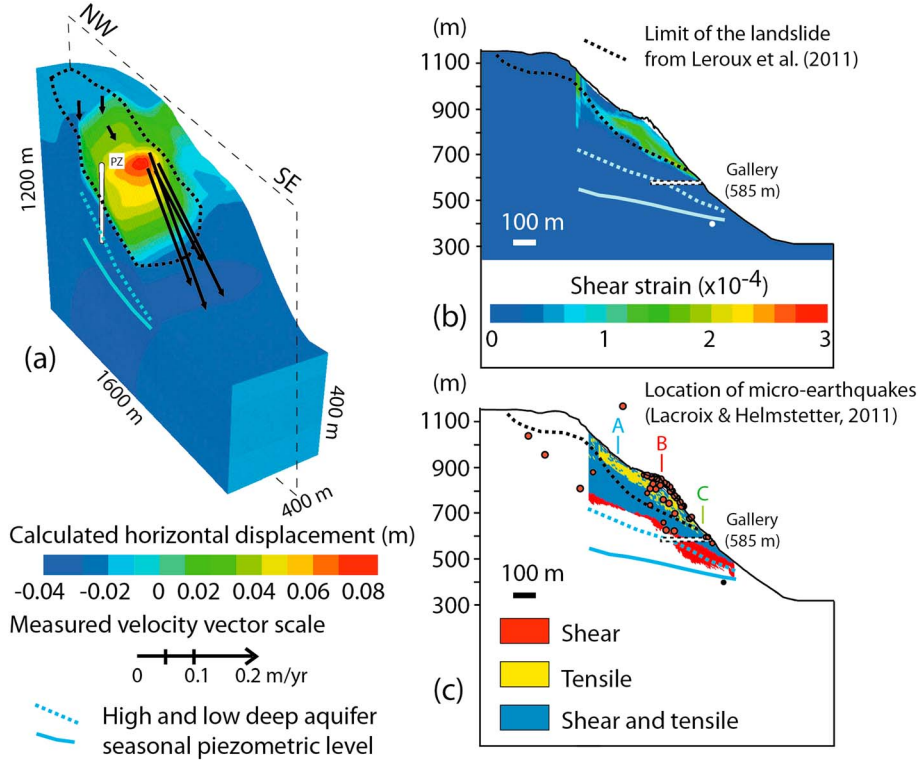
Figure 2. Comparison of model results to geodetic, geophysical imaging, and microseismic data. Three-dimensional views of (a) horizontal displacements, (b) shear strain, and (c) plastic rupture plotted on the NW-SE cross section in Figure 2a (indexes A, B, and C indicate the location of measured vertical profiles presented in Figure 3).
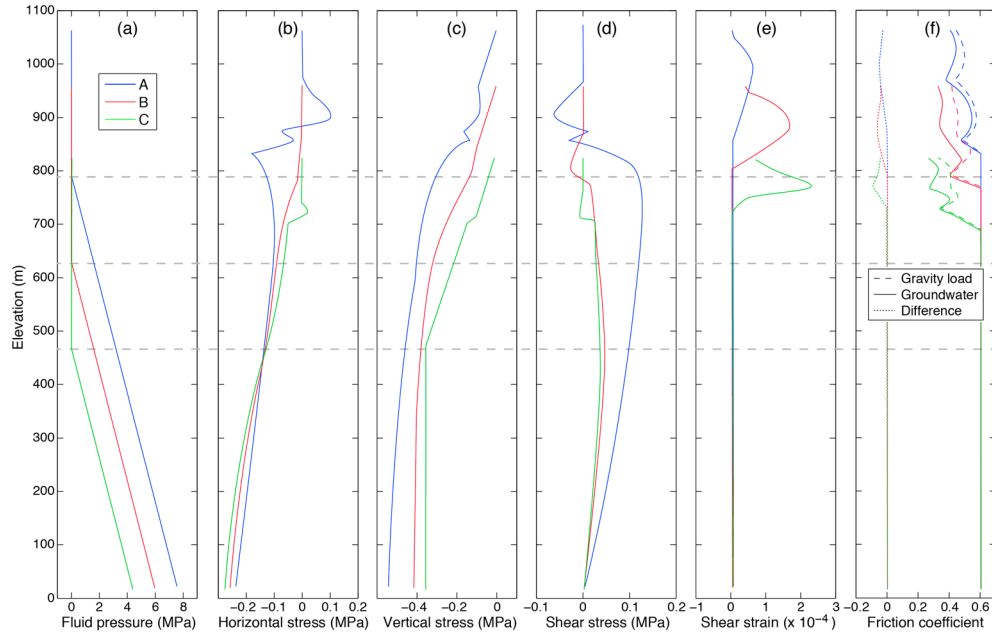

Figure 3. Vertical profiles of calculated changes in (a) fluid pressure, (b) total horizontal stress, (c) total vertical stress, (d) maximum shear stress, (e) shear strain, and (f) friction coefficient when the water table is increased and deformation stops varying. With this representation, we show the difference between the initial dry state and the final state with fluids. The location of the profiles is shown in Figure 2c. The blue profile (A) corresponds to the upstream part of the ruptured volume, the red (B) to the middle part (high-motion zone in the field, Figures 1a and 1b), and the green (C) to the downstream part. The horizontal dashed lines indicate the groundwater level for each profile. For the profiles of changes in friction coefficient in Figure 3f, we show the friction drop after the initial loading under gravity (dashed line) and after the groundwater table increase (solid line) and the difference between these two stages (dot).

increase of shear stress change is maintained, while inside the ruptured zone, the shear stress is reduced with values ranging from 0.01 to 0.06 MPa, and the horizontal stress is increased from 0.01 and 0.11 MPa at the downstream and upstream parts, respectively. The model indicates that the largest stress changes occur in the upstream part, where the fluid pressure is the highest in the deep aquifer. Consistently, the rerupturing illustrated by increased tensile and shear plastic zones (Figure 2c) is also associated with an additional reduction of friction on the order of 0.1 (Figure 3f). The highest reduction occurs downstream of the unstable volume, where the shear strain is the highest.

5. Discussion and Conclusions

[13] Although some seasonal variability of landslide deformation related to rainfall has been previously observed around the world for landslides close enough to their critical state, we show here with a simple hydromechanical model that a significant part of rupture can be driven by the mechanisms of stress transfer and friction weakening above and far from the water table. Our model reproduces all existing observations and shows that measured deformations and observed seismicity can be explained by the presence of a shallow weak damaged zone that is stable at dry conditions but can experience stress changes and shear-induced frictional weakening when the groundwater level varies during the long-term recharge, causing rerupturing. This result is consistent with the seismological study of *Helmstetter and Garambois* [2010], which showed that aseismic strain in the Séchilienne slope is dominant and localized in the deep saturated zone below the most seismogenic region situated in the unsaturated zone of the landslide. Thus, our study suggests a new physical interpretation of the concept of landslide activation by explaining how deep fluid pressures can cause stable damaged volume in a rock slope to become unstable as a result of stressing and gradual weakening during groundwater motions. Stress changes on the order of 0.01–0.11 MPa are found above the phreatic zone to initiate rerupturing of the landslide.

[14] Finally, this study reveals an unexpected alteration of the subsurface stress field and rock friction that leads to the rerupturing of the landslide above the phreatic zone, providing a reasonable explanation for the observed surface deformations and seismicity. It also shows that this stress alteration zone is only partly imaged by deep geophysical methods and seismic monitoring, which, in turn, present uncertainties. This may be correlated to the strong porosity increase [*Le Roux et al.*, 2011] mainly induced by the dilatant opening of preexisting and newly formed fractures in the pure-traction rupture zone that plays the role of a major attenuation zone in the available seismic tomographies. Our study has implications for landslides hazard, because it suggests that weak forcing from deep groundwater motions may reactivate stable or slowly moving landslides nested in the unsaturated zone and that current monitoring methods do not completely inform on the state of the active weakening zone, where catastrophic rupture may nucleate. This result is consistent with observations in other geological contexts, such as fluid injections into geological reservoirs [*Baisch et al.*, 2010] and fault zones [*Derode et al.*, 2013], where stressing due to fluid pressures produces deformation and rupture in the dry zone far from the source region, eventually triggering relatively large magnitude earthquakes. Such results are also crucial in defining mechanisms of strain partitioning and risk assessment in seismogenic regions where fluids are involved, such as earthquake faults, because landslides can be viewed as a useful natural analog for observing seismic and aseismic sliding [*Gomberg et al.*, 2011], and the possibility that stresses into stable regions could be modified close to an active fluid pressure source.

References

Baisch, S., R. Vörös, E. Rothert, H. Stang, R. Jung, and R. Schellschmidt (2010), A numerical model for fluid injection induced seismicity at Soultz-sous-Forêts, *Int. J. Rock Mech. Min. Sci.*, *47*(3), 405–413.

Cappa, F., and J. Rutqvist (2011), Modeling of coupled deformation and permeability evolution during fault reactivation induced by deep underground injection of CO_2, *Int. J. Greenhouse Gas Control*, *5*, 336–346, doi:10.1016/j.ijggc.2010.08.005.

Cappa, F., Y. Guglielmi, V. Merrien-Soukatchoff, J. Mudry, C. Bertrand, and A. Charmoille (2004), Hydromechanical modeling of a large moving rock slope inferred from slope levelling coupled to spring long-term hydrochemical monitoring: Example of the La Clapière landslide (Southern-Alps, France), *J. Hydrol.*, *291*(1–2), 67–90.

Derode, B., F. Cappa, Y. Guglielmi, and J. Rutqvist (2013), Coupled seismo-hydromechanical monitoring of inelastic effects on injection-induced fracture permeability, *Int. J. Rock Mech. Min. Sci.*, *61*, 266–274, doi:10.1016/j.ijrmms.2013.03.008.

Gaffet, S., Y. Guglielmi, F. Cappa, C. Pambrun, T. Monfret, and D. Amitrano (2010), Use of the simultaneous seismic, GPS and meteorological monitoring for the characterization of a large unstable mountain slope in the southern French Alps, *Geophys. J. Int.*, *182*, 1395–1410, doi:10.1111/j.1365-246X.2010.04683.x.

Gomberg, J., W. Schulz, P. Bodin, and J. Kean (2011), Seismic and geodetic signatures of fault slip at the Slumgullion Landslide Natural Laboratory, *J. Geophys. Res.*, *116*, B09404, doi:10.1029/2011JB008304.

Guglielmi, Y., J. M. Vengeon, C. Bertrand, J. Mudry, J. P. Follacci, and A. Giraud (2002), Hydrogeochemistry: An investigation tool to evaluate infiltration into large moving rock masses (case study of La Clapière and Séchilienne alpine landslides), *Bull. Eng. Geol. Environ.*, *61*, 311–324, doi:10.1007/s10064-001-0144z.

Guglielmi, Y., F. Cappa, and S. Binet (2005), Coupling between hydrogeology and deformation of mountainous rock slopes: Insights of La Clapière area (Southern-Alps, France), *C. R. Geosci.*, *337*, 1154–1163.

Helmstetter, A., and S. Garambois (2010), Seismic monitoring of Séchilienne landslide (French Alps): Analysis of seismic signals and their correlation with rainfalls, *J. Geophys. Res.*, *115*, F03016, doi:10.1029/2009JF001532.

Itasca Consulting Group (2006), FLAC³ᴰ—Fast Lagrangian Analysis of Continua in 3 Dimensions, Version 3.0, Five volumes, Itasca Consulting Group, Minneapolis.

Iverson, R. M. (2005), Regulation of landslide motion by dilatancy and pore pressure feedback, *J. Geophys. Res.*, *110*, F02015, doi:10.1029/2004JF000268.

Lacroix, P., and A. Helmstetter (2011), Localization of seismic signals associated with micro-earthquakes and rockfalls on the Séchilienne landslide, French Alps, *Bull. Seismol. Soc. Am.*, *101*(1), 341–353, doi:10.1785/0120100110.

Le Roux, O., D. Jongmans, J. Kasperski, S. Schwartz, P. Potherat, V. Lebrouc, R. Lagabrielle, and O. Meric (2011), Deep geophysical investigation of the large Séchilienne landslide (Western Alps, France) and calibration with geological data, *Eng. Geol.*, *120*, 18–31, doi:10.1016/j.enggeo.2011.03.004.

Meric, O., S. Garambois, D. Jongmans, M. Wathelet, J. L. Chatelain, and J. M. Vengeon (2005), Application of geophysical methods for the investigation of the large gravitational mass movement of Séchilienne, France, *Can. Geotech. J.*, *42*, 976–899.

Spillmann, T., H. Maurer, A. G. Green, B. Heincke, H. Willenberg, and S. Husen (2007), Microseismic investigation of an unstable mountain slope in the Swiss Alps, *J. Geophys. Res.*, *112*, B07301, doi:10.1029/2006JB004723.

Vallet, A., C. Bertrand, and J. Mudry (2013), Effective rainfall: A significant parameter to improve understanding of deep-seated rainfall triggering landslide—A simple computation temperature based method applied to Séchilienne unstable slope (French Alps), *Hydrol. Earth Syst. Sci. Discuss.*, *10*, 8945–8991.

Viesca, R. C., and J. R. Rice (2012), Nucleation of slip-weakening rupture instability in landslides by localized increase of pore pressure, *J. Geophys. Res.*, *117*, B03104, doi:10.1029/2011JB008866.

Willenberg, H., S. Loew, E. Eberhardt, K. F. Evans, T. Spillman, B. Heincke, H. Maurer, and A. G. Green (2008), Internal structure and deformation of an unstable crystalline rock mass above Randa (Switzerland): Part I—Internal structure from integrated geological and geophysical investigations, *Eng. Geol.*, *101*, 1–14.